

# THE CONTRIBUTION OF OIL PRODUCTION MECHANISMS AS DETERMINED BY A NOVEL CENTRIFUGING TECHNIQUE

by David P. Tobola, Phillips Petroleum Company

## ABSTRACT

A novel centrifuging procedure has been developed which permits the oil produced to be allocated between spontaneous imbibition and viscous displacement mechanisms. The new technique allows for spontaneous imbibition to occur within the centrifuge while at a very low rotational rate. Once the spontaneous imbibition process has ceased, the process is continued as a conventional centrifuge experiment with emphasis on attaining equilibrium conditions prior to increasing the rotational rate.

The oil recovery contribution for each production mechanism has been analyzed as a function of negative capillary pressure and wettability for a North Sea chalk. For a highly water-wet chalk sample, the spontaneous imbibition saturation endpoint and the viscous displacement saturation endpoint were very nearly the same, regardless of the capillary pressures investigated. Viscous displacement forces became significant only as the water-wetness of the sample decreased. At sufficient pressure, a less water-wet system could produce to a lower residual oil saturation when compared to a similar but highly water-wet system.

## INTRODUCTION

A new centrifuging technique was developed in an effort to determine the allocation of total oil production between the production components of spontaneous imbibition and viscous displacement. The new procedure allowed for spontaneous imbibition to occur within the centrifuge while it was spinning at a very low rate, thereby exerting a minimal negative capillary pressure force, typically -0.6 psi. The samples were wrapped in tissue and packed in sand, thereby allowing spontaneous imbibition to occur from any surface of the core sample, just as in a traditional table-top experiment. Once oil production was no longer observed, the centrifuge rate was increased to impose a gradient across the sample.

With the extended centrifuge technique, the spontaneous imbibition endpoint saturation (approximately  $P_c = -0.6$  psi) is equated to the  $P_c = 0$  cross-over point. Once equilibrium conditions are attained at this initial pressure gradient, the experiment continues as a traditional centrifuge run. Equilibrium conditions for this research were defined as no additional oil production observed for at least 48 hours.

## EXPERIMENTAL RESULTS

The extended centrifuging technique was utilized in determining the effect of wettability on the production mechanisms related to the negative capillary pressure characteristics of a North Sea chalk. A total of eight core samples were selected for this study. General properties of the core samples are presented in Table 1. Six of the core samples indicated a moderate-to-high degree of water-wetness and two appeared to be representative of low-to-moderately water-wet characteristics. The initial wetting states were based upon table-top spontaneous imbibition tests.

The initial rotation rate, yielding an approximate capillary pressure of -0.6 psi, was representative of the spontaneous imbibition endpoint and therefore equivalent to the point where capillary pressure equals zero. Subsequent capillary pressures investigated were approximately -2, -3, -4, -5, -7, and -10 psi. Actual pressures for each core sample varied slightly from these values due to minor differences in sample length. The incremental buildup in pressure permitted detailed information during the transitional segment of the negative capillary pressure curves. The collected data were analyzed by the methodology described by Hassler and Brunner (Reference 1). There are various methods of processing centrifuge data into capillary pressure information and each has its own inherent assumptions and limitations. This research was a comparative study among the data generated, therefore the main criteria to drawing conclusions from the generated data set was that all eight samples be analyzed by the same procedure. It was not the objective of this research to focus on the merit of any one specific analytical technique in comparison to another.

Amott-Harvey (Reference 2) Relative Displacement Index (RDI) values were determined from the centrifuge data to estimate a measure of wettability as defined by Equation 1.

$$RDI = \left[ \frac{\Delta(Sw)_{imbibition}}{\Delta(Sw)_{imbibition} + \Delta(Sw)_{viscous}} \right]_{Water} - \left[ \frac{\Delta(Sw)_{imbibition}}{\Delta(Sw)_{imbibition} + \Delta(Sw)_{viscous}} \right]_{Oil} \quad Eqn. 1$$

RDI was calculated using the highest capillary pressure measured during the experiment, approximately -10 psi, for the viscous displacement component of the equation. For the six highly water-wet samples, the negative capillary pressure had ceased to change and was approaching asymptotic behavior. For the two less water-wet samples, additional oil production may have been observed from the viscous displacement component if higher pressures had been attainable. Higher pressures would have resulted in their RDI values being reduced. None of the eight core samples was observed to spontaneously imbibe the oil phase, decane. Therefore, the RDI values reported are representative of the water index segment of the equation. The change in brine saturation from the initial value to the first centrifuge data point represents the amount attributable to spontaneous imbibition.

The design of the extended centrifuge experiments permitted the observed changes in saturation to be divided between the production mechanisms of spontaneous imbibition and forced viscous displacement. The production data from the experiments were analyzed in this manner to illustrate, for a given capillary pressure, what percentage of the observed production was attributable to each mechanism.

## DISCUSSION OF RESULTS

### Low-to-Moderately Water-Wet Samples

The negative capillary pressure data generated for the low-to-moderate water-wet core samples are illustrated in Figure 1, with capillary pressure being shown as a function of the calculated Hassler-Brunner inlet brine saturation. The RDI values calculated for these cores were 0.41 for Sample A and 0.54 for Sample B. Both cores were still in the transitional phase of the curve when the centrifuge run was terminated due to pressure limitations of the equipment. If a higher rotational rate had been attainable (i.e. a higher capillary pressure), the production due to viscous

displacement would have been greater, resulting in a lower RDI value than what was calculated.

Sample A demonstrated a very high air permeability of 33.4 md. While this permeability is not typical for the North Sea core samples, the value is believed to be valid. The air permeability was measured at different times by various individuals and the permeability did not change substantially. There was no visual evidence of fractures which may have influenced this parameter. This sample was also the least water-wet and was valuable for extending the wettability range being investigated.

### **Water-Wet Samples**

Figure 2 illustrates the data from the water-wet core data set, comprised of Samples C, D, and E, with all three core samples demonstrating an RDI of 0.88. The portion of the curve dominated by spontaneous imbibition is greater than the previous less water-wet core samples. The average production attributable to imbibition is approximately 88 percent of the total oil produced, with the remaining 12 percent due to viscous displacement. The viscous portion of the curves has a much steeper slope than the less water-wet samples.

### **Highly Water-Wet Samples**

Figure 3 illustrates the highly water-wet core subgroup with the highest RDI values. The RDI values were 0.91 for Sample F, 0.97 for Sample G, and 0.99 for Sample H. This wettability range exhibits the greatest change in saturation attributable to the spontaneous imbibition mechanism. The average production due to this mechanism was 96 percent of the total oil produced during the entire experiment, while viscous displacement accounted for 4 percent. Sample H, with the highest RDI of 0.99, demonstrates the greatest imbibition response and the least viscous response. For a highly water-wet system, the imbibition brine saturation endpoint is essentially the same as the viscous endpoint. After the spontaneous imbibition mechanism had ceased production, the viscous displacement portion of the negative capillary pressure curve was very nearly vertical.

### **Analysis of Production Mechanisms**

The design of the extended centrifuge experiments permitted the separation of the changes in saturation due to spontaneous imbibition and the changes in saturation due to viscous displacement. The contribution from each of these production mechanisms, plus the initial water volume present, made up the final water saturation within the core sample at a particular viscous force, i.e. capillary pressure. This type of analysis was performed as a function of wettability for the eight North Sea core samples investigated.

Figure 4 demonstrates the average trends in initial water saturation, the observed change in water saturation due to spontaneous imbibition, and the final water saturation ( $S_{wf}$ ), as a function of wettability, i.e. RDI. As noted earlier, there was no evidence of oil imbibition in any of the samples studied. Each of the lines represents the linear regression from the generated data for each of these categories. The initial water saturation was established by a centrifuging technique which incorporates core sample rotation and flipping in order to more equally distribute the fluids within the sample. There were no significant trends observed in the initial water saturation with RDI, for the core samples and the wettability range examined.

The change in water saturation due to spontaneous imbibition mechanism only did exhibit a trend with wettability. The more highly water-wet core samples exhibited a greater change in saturation than the lesser water-wet samples. The final water saturation, composed of the initial

water phase volume plus the imbibed water phase, are representative of the cross-over point ( $P_c$  equal to zero) on a capillary pressure curve.

Figure 5 is a composite of the viscous component trend lines developed for the capillary pressures investigated. The contribution toward total oil production from the viscous displacement mechanism increased most dramatically for the samples that were less than highly water-wet. This observation is consistent with the technical literature (Reference 2, 4, 5) which indicated that the maximum oil recovery was likely to occur as a system approached neutral wettability. This was likely due to the minimization of the interfacial forces that may disconnect and trap the oil phase. As the wettability approached the highly water-wet conditions, a significantly reduced benefit was observed from the viscous component of oil recovery.

Literature (Reference 2, 4, 5) suggests that in a strongly water-wet system, the water phase will tend to travel through the smaller pores, possibly bypassing some of the oil in the larger pores. The strong interfacial forces may disconnect and 'snap off' some of the oil. In a strongly oil-wet system, the tendency would be for the water to finger through the larger pores, thereby bypassing some of the oil. The neutral wettability case would have less tendency for water to bypass the oil and/or trap oil due to the oil ganglia remaining intact and thus being able to continue to contribute to oil production, thereby reducing the value of residual oil left behind after a water flood.

Figure 6 is a composite of the final water saturation trend lines representative of the capillary pressure and wettabilities investigated. For a system dominated by spontaneous imbibition (capillary pressure approximately equal to zero), the trend is for the final water saturation to increase as the water-wetness of the sample increases. However, when a viscous gradient is imposed, this trend will eventually reverse itself. The final water saturation trend line will pivot around a point representative of a constant final water saturation at an extremely high degree of water-wetness. This demonstrates that for a highly water-wet system, the spontaneous imbibition endpoint saturation is the same, or very nearly the same, as the viscous displacement saturation endpoint. This holds true where realistic field-type pressure gradients are being exerted on the system. If the pressure gradient were to be unrealistically high, then the final water saturation could be artificially inflated due to an extremely high capillary number. Exerting a realistic viscous gradient on a highly water-wet system, which is already at a spontaneous imbibition endpoint saturation, will not result in significant, if any, additional oil production.

## CONCLUSIONS

Based upon observations resulting from this research, the following conclusions were drawn.

1. For highly water-wet chalk samples, the dominant production mechanism will be spontaneous imbibition, with viscous displacement contributing only minimal incremental production.
2. For highly water-wet chalk samples, with an RDI value approaching unity, the spontaneous imbibition endpoint saturation and the viscous endpoint saturation are nearly the same.
3. For the water-wet core samples exhibiting an RDI value greater than 0.85 (six samples), the average oil recovery attributable to spontaneous imbibition was 92 percent of the total oil recovered for a system exposed to a maximum capillary pressure of approximately - 10 psi.

4. For a low-to-moderately water-wet chalk sample, viscous displacement has the potential of being the dominant production mechanism provided sufficient pressure forces exist within the system.
5. For the low-to-moderately water-wet core samples (two samples: RDI's of 0.41 and 0.54), the average oil recovery attributable to spontaneous imbibition was 47 percent of the total oil recovered for a system exposed to a maximum capillary pressure of approximately - 10 psi.
6. The contribution of viscous forces in oil recovery has the potential to be more significant in moderate and less-than-moderate water-wet systems than they may be for similar but highly water-wet systems, provided sufficient pressure forces exist within the system.

### Acknowledgments

The author would like to acknowledge Phillips Petroleum Company Norway and Co-venturers, including Fina Exploration Norway S.C.A., Norsk Agip A/S, Elf Petroleum Norge AS, Norsk Hydro Produksjon a.s, TOTAL Norge A.S, Den norsk stats oljeselskap a.s, Elf Rex Norge A/S and Saga Petroleum a.s for their financial support and permission to publish this paper. The opinions expressed are those of the author and do not necessarily represent those of Phillips Petroleum Company Norway and Co-venturers.

### References

1. Hassler, G. L. and Brunner, E.: "Measurement of Capillary Pressures in Small Core Samples," *Trans. AIME* (1945), Vol. 160, 114-123.
2. Amott, E.: "Observations Relating to the Wettability of Porous Rock," *Trans. AIME* (1959), Vol. 216, 156-162.
3. Leverett, M. C.: "Capillary Behavior in Porous Solids," *Trans. AIME* (1941), Vol. 142, 152-169.
4. Anderson, W. G.: "Wettability Literature Survey - Part 6: The Effect of Wettability on Waterflooding," *JPT* (Dec. 1987), 1605-1621.
5. Anderson, W. G.: "Wettability Literature Survey - Part 4: The Effect of Wettability on Capillary Pressure," *JPT* (Oct. 1987), 1283-1300.
6. Anderson, W. G.: "Wettability Literature Survey - Part 1: Rock/Oil/Brine Interactions and the Effects of Core Handling on Wettability," *JPT* (Oct. 1986), 1125-1144.

**Table 1 - Core Sample Description**

<b>Core</b>	<b>K, air (md)</b>	<b>Porosity, % PV</b>	<b>RDI (Water Index)</b>
A	33.43	26.8	0.41
B	5.40	34.9	0.54
C	3.71	34.1	0.88
D	4.55	36.4	0.88
E	0.93	20.8	0.88
F	0.28	17.4	0.91
G	1.58	36.8	0.97
H	2.24	28.7	0.99

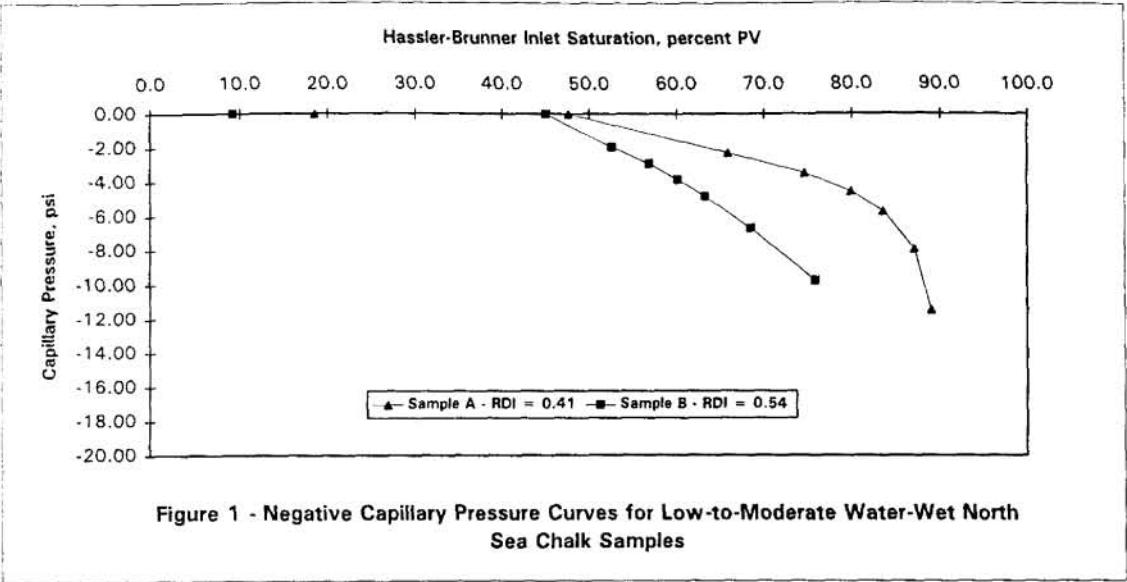


Figure 1 - Negative Capillary Pressure Curves for Low-to-Moderate Water-Wet North Sea Chalk Samples

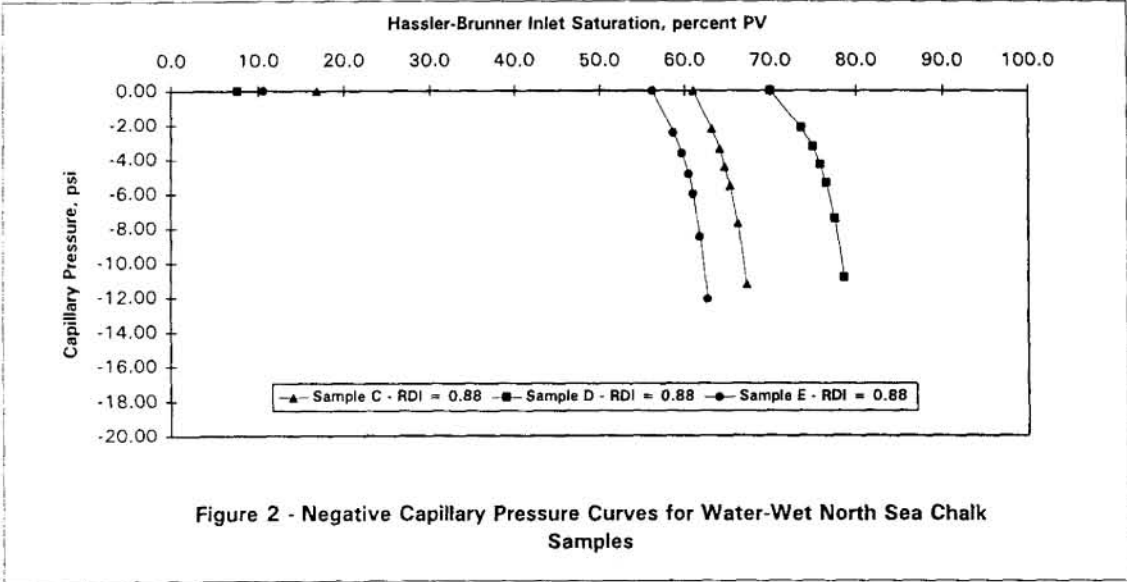


Figure 2 - Negative Capillary Pressure Curves for Water-Wet North Sea Chalk Samples

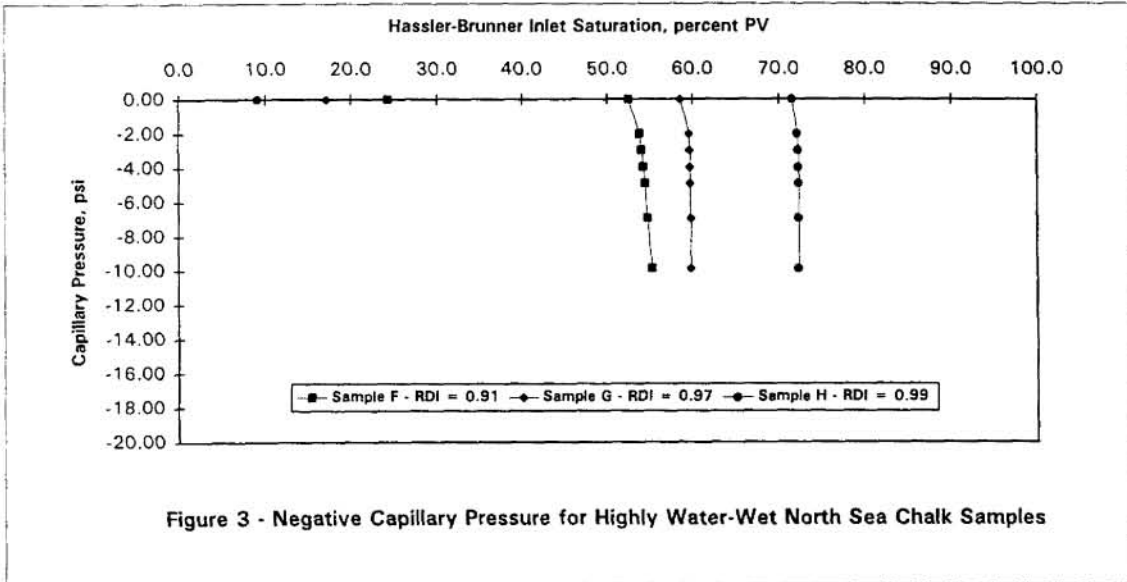


Figure 3 - Negative Capillary Pressure for Highly Water-Wet North Sea Chalk Samples

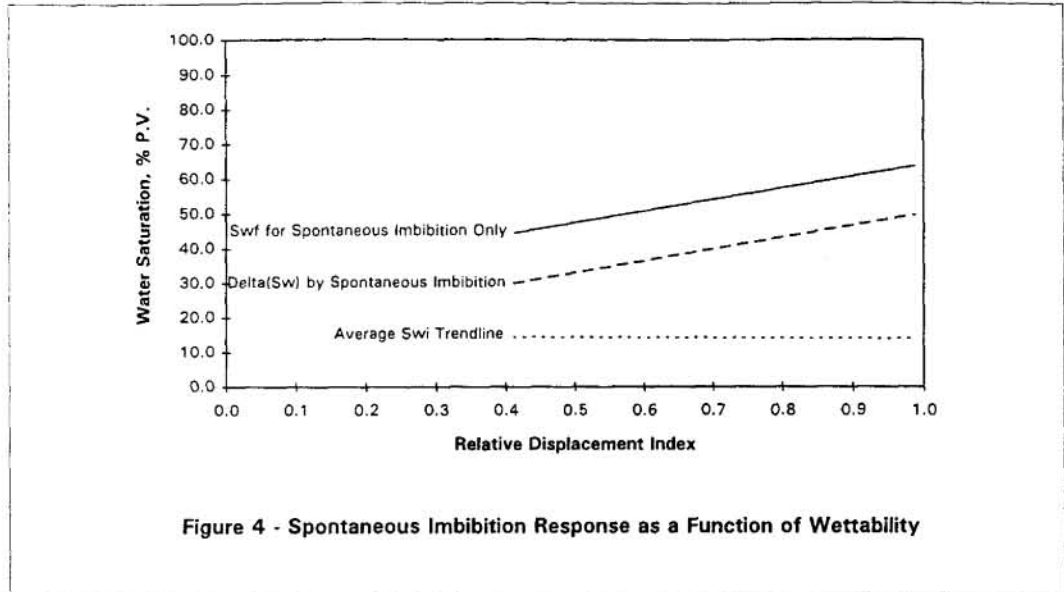


Figure 4 - Spontaneous Imbibition Response as a Function of Wettability

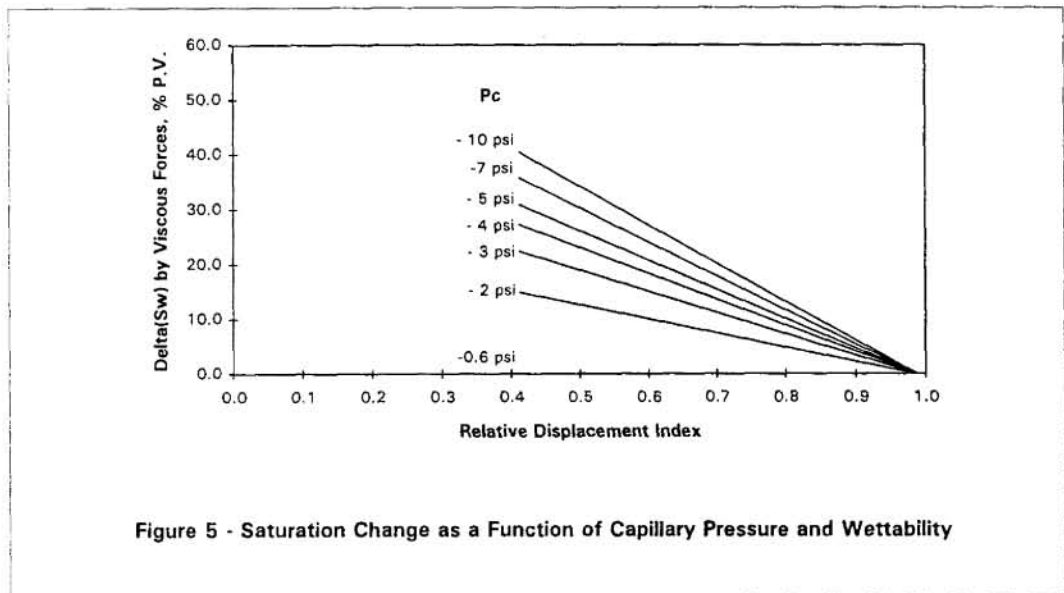


Figure 5 - Saturation Change as a Function of Capillary Pressure and Wettability

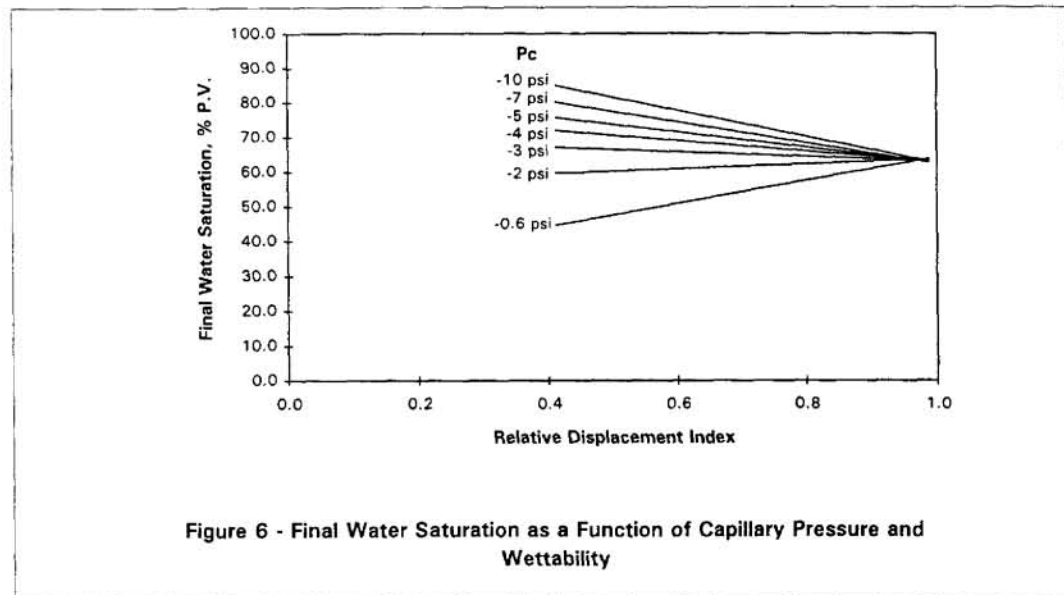


Figure 6 - Final Water Saturation as a Function of Capillary Pressure and Wettability